American Mineralogist, Volume 78, pages 285–297, 1993

# Synthesis, stability, and properties of $Al_2SiO_4(OH)_2$: A fully hydrated analogue of topaz

**B. Wunder**
Institut für Mineralogie, Ruhr-Universität Bochum, 4630 Bochum, Germany
**D. C. Rubie, C. R. Ross II**
Bayerisches Geoinstitut, Universität Bayreuth, 8580 Bayreuth, Germany
**O. Medenbach**
Institut für Mineralogie, Ruhr-Universität Bochum, 4630 Bochum, Germany
**F. Seifert**
Bayerisches Geoinstitut, Universität Bayreuth, 8580 Bayreuth, Germany
**W. Schreyer**
Institut für Mineralogie, Ruhr-Universität Bochum, 4630 Bochum, Germany

## Abstract

The OH end-member of the F-OH topaz solid-solution series, with a composition close to $Al_2SiO_4(OH)_2$, has been synthesized at pressures between 55 and 100 kbar and temperatures up to 1000 °C from gels and crystalline starting materials. The results of single-crystal X-ray diffraction [space group *Pbnm*, $a = 4.724(3)$ Å, $b = 8.947(7)$ Å, $c = 8.390(8)$ Å] show close agreement with the structure of F-rich topaz but a nearly pure dilatation of both the $^{[6]}$Al (5%) and the $^{[4]}$Si (1.5%) sites; the distortion parameters of these sites were slightly affected. Optical properties are $n_x \parallel a = 1.700(1)$, $n_y \parallel b = 1.701(1)$, $n_z \parallel c = 1.703(1)$, $\Delta n = 0.0040(5)$, and $2V_\gamma = 28(2)°$. In the infrared spectrum, the OH-stretching vibration is split into two bands at 3600 and 3520 $cm^{-1}$. This synthetic phase, referred to in this paper as "topaz-OH", breaks down to kyanite + $H_2O$ above 750 °C at 60 kbar and above 1050 °C at 90 kbar of $H_2O$ pressure. Toward lower pressures and temperatures its stability field is limited by assemblages with diaspore, coesite, and phase Pi of the probable composition $Al_3Si_2O_7(OH)_3$. It is suggested that "topaz-OH" may form in subducting slabs as a transient phase at depths of about 175 km.

## Introduction

The mineral topaz, a fluorine aluminum silicate of ideal composition $Al_2SiO_4F_2$, has long been known to exhibit partial OH-F substitution in the anionic F site (e.g., Pardee et al., 1937; Rosenberg, 1967; Ribbe and Rosenberg, 1971), which affects its crystallographic (Zemann et al., 1979), physical (Ribbe and Gibbs, 1971), and thermodynamic properties (Barton, 1982). A summary of the crystal chemistry of topaz is given by Ribbe (1982a).

In natural topaz, the observed OH for F substitution is limited to less than ~30 mol% (e.g., Pardee et al., 1937). In the system $Al_2O_3$-$SiO_2$-$H_2O$-$AlF_3$, synthesis of more OH-rich topaz [to OH/(OH + F) slightly above 0.5] has been reported (Rosenberg, 1972), but it is not clear whether the crystalline products correspond to the ideal $Al_2SiO_4F_{2-x}OH_x$ join and whether they represent metastable phases. The maximum amount of OH substitution obtained by Barton (1982) in reversed experiments using crystalline starting materials was $X_{OH} = OH/(OH + F) = 0.173$ at $P_{H_2O} = 1$ kbar.

It has been argued (Gebert and Zemann, 1965; Barton, 1982) that this limited substitution is due to proton-proton avoidance and that, therefore, the maximum theoretically possible OH/(OH + F) ratio should be 0.5. The maximum substitution would require at least partial F-OH ordering on the anionic site and might lead to a decrease in symmetry from the orthorhombic *Pbnm* space group of pure fluorine topaz. Such a lowering of symmetry to *P*1 (ascribed to a growth effect) has actually been observed by optical and X-ray methods in OH-bearing topaz by Akizuki et al. (1979) and Parise et al. (1980). On the other hand, Abbott (1990) has recently predicted, on the basis of energy calculations, that an OH end-member of topaz might actually exist because of stabilization by H bonding.

The experimental work by Barton (1982) indicated that increasing $H_2O$ pressures and decreasing temperatures lead to an increase in the OH/(OH + F) ratio of topaz in equilibrium with an $Al_2SiO_5$ aluminum silicate and a fluid. Provided the activity-composition relationships are known along the join hydroxyl topaz–fluorine topaz, its composition in the assemblage with an aluminum silicate could serve as a sensitive indicator of F activity in a co-

0003–004X/93/0304–0285$02.00

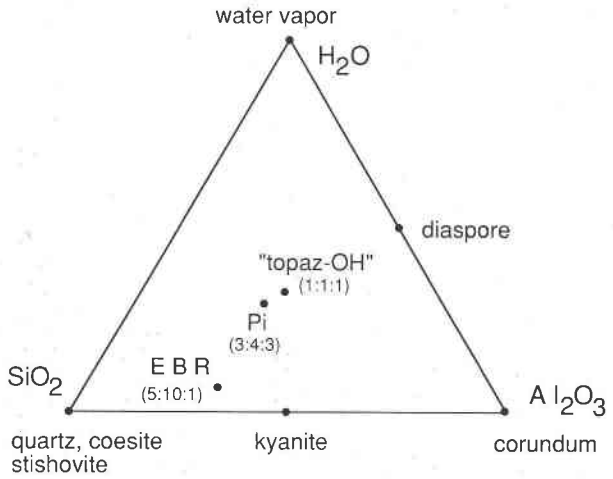


Fig. 1. Chemography of high-pressure phases in the system $Al_2O_3$-$SiO_2$-$H_2O$. EBR designates the phase described by Eggleton et al. (1978). Pi stands for phase Pi, first synthesized and named piezotite by Coes (1962); cf. also Wunder and Schreyer (1991). For the ternary phases, the molar proportions $Al_2O_3$:$SiO_2$:$H_2O$ are given in parentheses. Note the colinearity of the $SiO_2$ polymorphs, phase Pi, "topaz-OH," and diaspore, as well as that of kyanite with "topaz-OH" and $H_2O$.

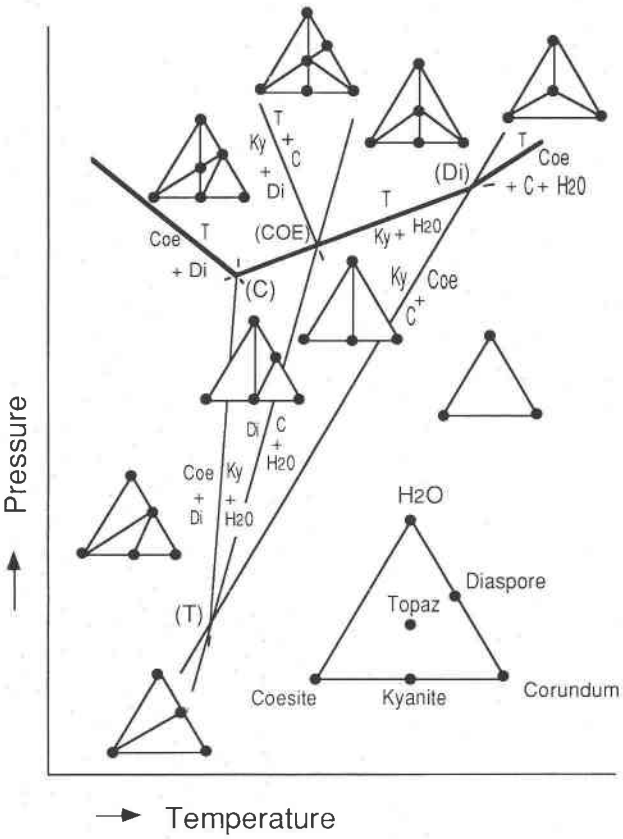


Fig. 2. Topological analysis of one of the four possible networks of maximum closure formed by the phases "topaz-OH" (T), kyanite (Ky), $H_2O$ (V), corundum (C), coesite (Coe), and diaspore (Di). Invariant points are characterized by the absent phase (given in parentheses), e.g., the point designated (C) is the one formed by the phases "topaz-OH," kyanite, $H_2O$, coesite, and diaspore. The stability field of "topaz-OH" is delineated by the heavier univariant lines.

existing fluid. Barton (1982) developed such a model on the basis of the proton-avoidance rule and therefore implied that a pure OH end-member of the topaz solid-solution series cannot be stable.

During a reconnaissance investigation of the system MgO-$Al_2O_3$-$SiO_2$-$H_2O$ we have recently synthesized large crystals (up to 200 $\mu$m in length) of the OH end-member of topaz at 100 kbar and 1000 °C (Medenbach et al., 1990). Because of the significance of this observation for the crystallographic and thermodynamic properties of topaz as mentioned above, the stability of the phase and some of its properties are reported in this paper. We are aware of the nomenclature problem created by the fact that the new synthetic phase, hitherto not described as a natural mineral, cannot be given a proper mineralogical name. Nevertheless, because of the close chemical and crystal structural relationship with the familiar mineral topaz, it is referred to in the remainder of the paper as "topaz-OH." Although this nomenclature is not standard, it is a convenient and efficient means of conveying chemical and structural information about the phase by direct analogy with a well-known mineral.

## Topological analysis of phase relations in the system $Al_2O_3$-$SiO_2$-$H_2O$ at high pressures

Phase relations in this system have been calculated by Delany and Helgeson (1978) up to 50 kbar and 600 °C. They showed that at elevated pressures (>30 kbar) and elevated temperatures (>400 °C) coesite ($SiO_2$), kyanite ($Al_2SiO_5$), diaspore (AlOOH), and corundum ($Al_2O_3$) may be the only stable solid phases. The thermodynamic data extracted by Berman (1988) from experimentally determined phase relations are consistent with this notion. However, in a complete topological analysis, the following other phases have to be considered in addition: (1) The new phase "topaz-OH," ideally $Al_2SiO_4(OH)_2$. (2) Phase Pi. In the original synthesis of this phase at 40–45 kbar, ~700 °C, as reported by Coes (1962), this compound was called "piezotite," and its formula was given as $Al_2O_3 \cdot 3SiO_2$, but it later was corrected to $Al_3Si_2O_7(OH)_3$ (Vaughan and Berman, 1963). A confirmation of this formula, as well as new data on stability and properties of this phase, is described elsewhere (Wunder and Schreyer, 1991). In order to avoid nomenclature problems we use the term "phase Pi" in allusion to the name applied by Coes (1962). (3) $Al_5Si_5O_{17}(OH)$. The synthesis of this phase has been reported by Eggleton et al. (1978) at pressures >100 kbar and at temperatures near 1000 °C. This phase has not been encountered in our study. In the analysis that follows, phase Pi and $Al_5Si_5O_{17}(OH)$ will not be taken into account. The chemography of the phases is depicted in Figure 1.

**TABLE 1.** Selected synthesis experiments and reversals bearing on the stability of "topaz-OH"

| Starting material | Composition (+$H_2O$) | Conditions kbar/°C/h | Products (+$H_2O$ vapor) |
|---|---|---|---|
| Gel | $4MgO \cdot 9Al_2O_3 \cdot 8SiO_2$ | 90/900/10 | topaz, MgMgAl-P, diaspore |
| Gel | $4MgO \cdot 3Al_2O_3 \cdot 6SiO_2$ | 100/1000/15.5 | topaz*, pyrope, melt? |
| Gel + $SiO_2$ glass | $Al_2SiO_5 + SiO_2$** | 100/950/17.5 | topaz†, stishovite |
| Gel + $SiO_2$ glass | $Al_2SiO_5 + SiO_2$** | 100/900/16 | topaz‡, stishovite, unknown phase |
| Gel | $Al_2SiO_5$ | 80/1000/12 | kyanite |
| Gel | $Al_2SiO_5$ | 90/1000/17 | topaz§ |
| Ky + Top | $Al_2SiO_5$ | 85/1000/16 | kyanite$^+$, topaz$^-$ |
| Ky + Top | $Al_2SiO_5$ | 90/800/15 | topaz$^+$, kyanite$^-$ |
| Ky + Top | $Al_2SiO_5$ | 80/700/36 | topaz$^+$, kyanite$^-$ |
| Ky + Top | $Al_2SiO_5$ | 70/700/16 | topaz$^+$, kyanite$^-$ |
| Ky + Top | $Al_2SiO_5$ | 60/700/16 | topaz$^+$, kyanite$^-$ |
| Ky + Top | $Al_2SiO_5$ | 55/700/16 | topaz$^+$, kyanite$^-$ |
| Ky + Top | $Al_2SiO_5$ | 50/700/24 | topaz$^-$, kyanite$^+$ |
| Top + Pi + Dia + Coe | $3Al_2O_3 \cdot 4SiO_2$ | 55/500/18 | Pi$^+$, topaz, diaspore, coesite$^-$ |
| Gel | $Al_2SiO_5$ | 55/400/24 | diaspore, coesite |
| Gel | $Al_2SiO_5$ | 50/1000/48 | kyanite |
| Gel | $Al_2SiO_5$ | 50/900/48 | kyanite |
| Gel | $Al_2SiO_5$ | 50/700/48 | kyanite |
| Gel | $Al_2SiO_5$ | 50/600/72 | diaspore, Pi, little coesite |

*Note:* In the product column, growth and diminution of a phase relative to the concentration in the starting materials indicated by the + and − signs, respectively. Abbreviations: Pi = phase Pi $Al_3Si_2O_7(OH)_3$ (see text), MgAlAl-P = pumpellyite-(Mg) (Schreyer et al., 1991). In all the experiments, the amount of $H_2O$ added was about 20 wt%. The last seven experiments have been performed in a piston-cylinder press at the University of Bochum, the others in a multianvil press at Bayreuth.

* Used for single-crystal structure analysis, composition (6O, 2H) $Al_{2.07}Si_{0.95}O_4(OH)_2$.

** In the proportions (by weight) $5Al_2SiO_5$:$1SiO_2$.

† Composition (6O) $Al_{1.99}Si_{0.99}O_{3.93}(OH)_{2.07}$.

‡ Sample UHP 479, used for powder X-ray diffraction and IR spectroscopy, composition (6O) $Al_{1.95}Si_{1.04}O_4(OH)_{2.00}$.

§ Sample UHP 270, used for powder X-ray diffraction, IR spectroscopy, and Rietveld refinement.

Four topologies of nets of maximum closure (Day, 1972) are possible for the chemography of the six phases topaz, corundum, kyanite, diaspore, coesite, and $H_2O$ vapor, but only one of them can be oriented with respect to pressure and temperature, on the basis of thermodynamic data by Berman (cf. Fig. 2).

Of the reactions displayed in Figure 2, only the Di = C + V and Coe + Di = Ky + V equilibria have been established previously (cf. Berman, 1988). The equilibrium among topaz, kyanite, and vapor will be reported in this paper, and inferences on the position of the topaz = coesite + diaspore reaction will be made. There is no evidence yet for the postulated Ky = Coe + C reaction, but thermodynamic data indicate that, if it is a stable reaction at all, it must have a positive slope, with Coe + C being the high-temperature, low-pressure assemblage. Note that the sign of the slope will be reversed as soon as coesite is replaced by stishovite as the stable form of silica at pressures above some 90 kbar (cf. unpublished data by Liu as quoted in Eggleton et al., 1978). On the other hand, it should be pointed out that the two invariant points, namely Di and T, interconnected by the kyanite = coesite + corundum reaction, might be metastable because of incoming melt or stishovite and the additional crystalline ternary hydrous phase Pi (see above), respectively.

## EXPERIMENTAL METHODS

### Starting materials

Starting materials for the synthesis of topaz were gels of various compositions prepared according to the method described by Hamilton and Henderson (1968). For bracketing the topaz = kyanite + $H_2O$ reaction, an 8:1 mixture (by weight) of synthetic kyanite and synthetic topaz was used. Kyanite was prepared at 50 kbar, 700 °C, for 24 h (Table 1), again using a gel of appropriate composition as starting material. For experiments with excess $SiO_2$, a mixture of the $Al_2SiO_5$ gel and quartz (Heraeus Q-113, 99.99% purity) in the proportion 5:1 (by weight) was used.

### High-pressure experiments

High pressure synthesis and phase equilibrium experiments were performed using a uniaxial-split-sphere apparatus (Ito et al., 1984). The tungsten carbide anvils (Toshiba grade F) had a truncation edge length of 11 mm. Samples and excess $H_2O$ were cold-welded into Au capsules with either a 2- or a 3-mm diameter. Sample assemblies were octahedra, with an 18-mm edge length, consisting of semisintered MgO (+5% $Cr_2O_3$); preformed 5 × 3 mm pyrophyllite gaskets were used. The sample pressure was calibrated as a function of oil pressure using transitions in Bi at room temperature and by reversing the quartz + coesite, coesite + stishovite, and $\alpha Fe_2SiO_4$ + $\gamma Fe_2SiO_4$ equilibria at 1000 °C. A graphite heater with a variable wall thickness was used (Canil, 1991) in order to reduce the temperature gradient across the sample to <20 °C (Kanzaki, 1987). Temperature was monitored using a Pt-Pt10%Rh thermocouple and in phase equilibrium experiments was controlled to ±2 °C. The thermocouple emf was not corrected for the effect of pressure.

Experiments up to 55 kbar were carried out in a piston-

cylinder press (Boyd and England, 1960) at the University of Bochum. Starting materials and excess $H_2O$ were sealed into Au capsules with a length of nearly 10 mm. A mantled chromel-alumel thermocouple was used for temperature control and measurement. The Au capsule and the thermocouple were positioned in a NaCl pressure cell, type II, as depicted by Massonne and Schreyer (1986).

### Microprobe analyses

Microprobe analyses were performed by a Camebax electron microprobe at the University of Bochum and a Cameca SX 50 microprobe at Bayerisches Geoinstitut, Bayreuth. Synthetic pyrope ($Mg_3Al_2Si_3O_{12}$, Bochum) and natural orthoclase ($KAlSi_3O_8$, Bayreuth) served as standards.

### X-ray methods

For lattice constant determination, the samples were mixed with NBS Si ($a$ = 5.42081 Å for $\lambda_{CuK\alpha_1}$ = 1.54046 Å), and data from 15 to 139° 2$\theta$ were collected for unit-cell refinement on a Stoe STADIP powder diffractometer in transmission mode. Peak positions were determined by fitting modified Lorentzian profiles (Pyrros and Hubbard, 1983) to the observable reflections and then applying a linear internal standard correction based upon the positions of the Si peaks. Diffraction data for Rietveld refinement were collected from 18 to 140° 2$\theta$ in the same way, but without Si. Single-crystal photographs were taken by a Weissenberg camera using Ni-filtered Cu$K\alpha$ radiation and by a Stoe precession camera with Zr-filtered Mo$K\alpha$ radiation. Long exposure times (up to 7 d) were chosen to detect possible violations of space group *Pbnm*.

For the structure determination a crystal with dimensions 30 × 60 × 100 $\mu$m was selected from an experiment on the composition $4MgO \cdot 3Al_2O_3 \cdot 6SiO_2 + H_2O$ (Table 1), mounted on a Syntex-R3 four-circle diffractometer and aligned optically. Intensities of reciprocal lattice points (1563) to $0 \le h \le 9$, $0 \le k \le 16$, $-15 \le l \le 15$, and $2\theta \le 75°$ intensities were measured in a Wyckoff scan mode using graphite-monochromatized Mo$K\alpha_1$ radiation. Three out of every 50 peaks were periodically monitored as reference values. The intensities were corrected for Lorentz and polarization effects, scaled using the intensities of the reference peaks, and merged according to the symmetry restrictions of the Laue group *mmm* ($R_{merge}$ = 2.4%). This procedure resulted in 984 symmetrically independent structure amplitudes. The refinement was done with the program SHELX76 (Sheldrick, 1976). For the structure refinement 900 structure amplitudes with $|F| \ge 3\sigma(|F|)$ were used. The data were refined using statistical $(1/\sigma_F^2)$ weights. Neutral atom scattering factors (International Tables) were used. The structure reported by Zemann et al. (1979) was used as a starting point for the crystal structure refinement of "topaz-OH," substituting O for F. It refined to $R$ = 0.049 ($R_w$ = 0.045) with anisotropic temperature factors and without H atoms. After convergence, a difference Fourier map was generated and examined in an attempt to locate the H associated with the stoichiometric OH, as well as to evaluate the possibility that some of the Si deficiency in the chemical analysis was caused by $Si^{4+}$ for $4H^+$ (hydrogarnet substitution); the difference Fourier map was, however, featureless.

### Optics

The indices of refraction, the morphological data, and the twin relationships have been measured using a microrefractometer spindle stage. As the determination of small optical axial angles from extinction curves is not very sensitive, the crystal was first oriented by means of the spindle-stage technique and subsequently remounted with its $n_y$ parallel to a second spindle. This straightforward method was described by Medenbach (1985); it allows a very precise direct determination of $2V$ values. In addition, the birefringence was measured independently using a tilting compensator.

### Infrared spectra

The infrared spectra of synthetic "topaz-OH" and natural F-rich topaz were recorded with a Perkin-Elmer 325 spectrometer in transmission mode. The samples were prepared from homogenized mixtures of 1 mg of finely ground topaz and 400 mg of KBr as embedding material (dried at 120 °C for 24 h). A pure KBr pellet served as a reference.

## Synthesis and stability

"Topaz-OH" was first recognized in explorations on the system $MgO$-$Al_2O_3$-$SiO_2$-$H_2O$ at 90–100 kbar, 900–1000 °C, in which it coexisted with pumpellyite-(Mg) (cf. Schreyer et al., 1991) and diaspore or pyrope, respectively (cf. Table 1). Subsequently, we concentrated the study on the limiting system $Al_2O_3$-$SiO_2$-$H_2O$, using both gels and crystalline starting materials and excess $H_2O$. "Topaz-OH" was found to form easily from both amorphous and crystalline starting materials over a wide range of conditions of high pressure and moderate temperatures (Table 1, Fig. 3), whereas at higher temperatures and lower pressures, kyanite was formed, even when starting from crystalline kyanite + "topaz-OH" mixtures. Thus, the reaction "topaz-OH" = kyanite + $H_2O$ has been bracketed reversibly between about 60 and 100 kbar, and it passes through the approximate $P$-$T$ coordinates 1000 °C at 87.5 kbar and 700 °C at 52.5 kbar (Fig. 3). In order to test the compatibility of topaz with $SiO_2$, an experiment at 950 °C, 100 kbar, was performed with excess $SiO_2$ (Table 1). The result was "topaz-OH" and stishovite.

Phase relations at the low-pressure, low-temperature end of the "topaz-OH" stability field are not yet clear. A synthesis experiment starting from gel, at 55 kbar, 400 °C, yielded no topaz but, instead, diaspore + coesite. Unless a nucleation barrier exists for "topaz-OH," this might indicate that the low-temperature equivalent of topaz is formed by this assemblage through a reaction diaspore + coesite = "topaz-OH." At low pressures and intermediate temperatures, the phase Pi appears. It grows from a mixture of seeded topaz + diaspore + coesite at 55 kbar, 500

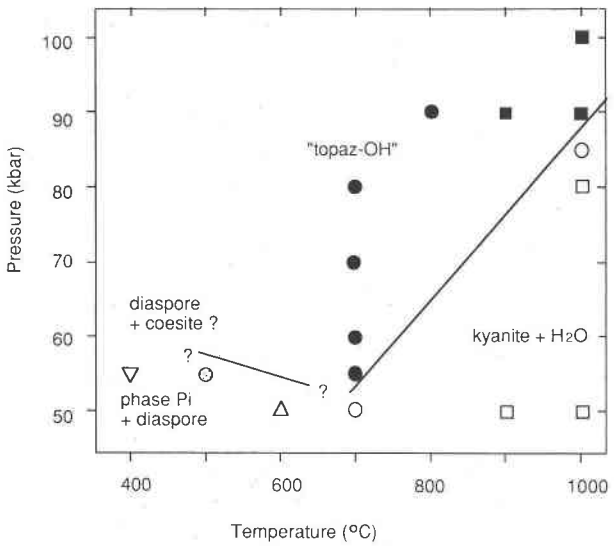


Fig. 3. *P-T* conditions of synthesis and reversed experiments bearing on the stability of "topaz-OH" (cf. Table 1). Triangles and squares refer to gel starting materials and circles to seeded crystalline starting materials. Filled symbols = growth of topaz; open circles and squares = kyanite; stippled circle = phase Pi; triangle = diaspore + phase Pi; inverted triangle = coesite + diaspore. The boundary lines give the summary of phase relations of "topaz-OH." Relations depicted at low temperatures and low pressures are tentative (see also Wunder and Schreyer, 1991). For data see Table 1.

°C, according to either reaction "topaz-OH" + coesite = phase Pi or diaspore + coesite = phase Pi. Phase relationships in this *P-T* part of the system are presently under more detailed investigation (Wunder and Schreyer, 1991, and in preparation).

Comparing these results to the topological analysis presented above (cf. Fig. 2) and neglecting the phase Pi, we note that the overall phase relations are consistent with that analysis, but that the invariant point labeled *C* at the intersection at the reactions topaz = kyanite + vapor, coesite + diaspore = topaz, and coesite + diaspore = kyanite + vapor is obviously at a higher level of stability through the stable formation of the phase Pi at these *P-T* conditions.

## Properties

### Chemistry

The average of 69 individual microprobe analyses at Bochum of crystals grown at 950 °C and 100 kbar for 17.5 h on the $Al_2SiO_5$ + excess $SiO_2$ + $H_2O$ composition gave $Al_2O_3$: 56.27 (±0.67), $SiO_2$: 33.05 (±0.55), and $H_2O$ (by difference): 10.68 (±0.47) wt%, to be compared with the theoretical composition $Al_2SiO_4(OH)_2$ with $Al_2O_3$ = 56.63, $SiO_2$ = 33.37 and $H_2O$ = 10.00 wt%. The structural formula $Al_{1.99}Si_{0.99}O_{3.93}(OH)_{2.07}$ (calculated on the basis of six O atoms) corresponds to the ideal formula $Al_2SiO_4(OH)_2$ within the precision of the measurements. In particular, it should be noted that the Al/Si ratio observed corresponds to the predicted value. The OH content calculated will heavily depend on the analytical total and, therefore, is intrinsically uncertain.

Analysis of a similar product (900 °C, 100 kbar, excess $SiO_2$) on the Bayreuth microprobe yielded $Al_2O_3$: 55.2 (±0.2), $SiO_2$: 34.8 (±0.2) wt% and a formula (on the basis of six O atoms) $Al_{1.95}Si_{1.04}O_4(OH)_{2.00}$, whereas the analyses of the crystals used for single-crystal X-ray diffraction yielded (on the Bochum microprobe) a formula (on the basis of six O atoms and two OH) $Al_{2.07}Si_{0.94}O_4(OH)_2$. There is evidence for slight chemical variability of "topaz-OH" with respect to the Al/Si ratio, and also possibly the $H_2O$ content, both between different samples and within a single sample, but without an independent analysis for structural $H_2O$ its variation could not be assessed.

**Table 2.** List of powder diffraction lines with relative intensities >20% in "topaz-OH" pattern

| *hkl* | *d* (Å) | $I/I_o$ (%) |
|---|---|---|
| 111 | 3.744 | 64 |
| 120 | 3.247 | 68 |
| 022 | 3.065 | 27 |
| 112 | 2.967 | 100 |
| 130 | 2.520 | 22 |
| 103 | 2.415 | 25 |
| 023 | 2.378 | 55 |
| 123 | 2.124 | 66 |
| 220 | 2.089 | 35 |
| 114 | 1.881 | 26 |
| 133 | 1.876 | 27 |
| 232 | 1.695 | 24 |
| 233 | 1.546 | 22 |
| 153 | 1.436 | 37 |
| 250 | 1.425 | 21 |
| 006 | 1.405 | 27 |
| 303 | 1.374 | 40 |

*Note:* "Topaz-OH" synthesized from gel of stoichiometric composition + $H_2O$ (sample UHP270 of Table 1).

### X-ray powder data

Two samples were chosen for detailed powder diffraction analysis, one synthesized from $Al_2SiO_5$ gel + $H_2O$ composition (i.e., ideal "topaz-OH") at 90 kbar/1000 °C (UHP 270), and the second from $Al_2SiO_5$ gel, $SiO_2$ glass (in the weight proportions 5:1) + $H_2O$ at 100 kbar and 900 °C (UHP 479). The first sample was 100% topaz, whereas the second sample was ~95% topaz with traces of stishovite and another as-yet unidentified phase.

The strongest powder diffraction lines of the UHP 270 sample ("topaz-OH" on composition) are reported in Table 2. The full data set has been submitted to International Centre for Diffraction Data for inclusion in the JCPDS Powder Diffraction File. Unit-cell parameters refined from peak positions in both the UHP 270 and the excess $SiO_2$ sample (UHP 479) are given in Table 3, along with (for comparison) the unit-cell parameters determined for the single crystal of this study.

### X-ray single-crystal structure analysis

Only in the experiment on the composition $4MgO \cdot 3Al_2O_3 \cdot 6SiO_2$ + $H_2O$ at 1000 °C and 100 kbar for 15.5

**TABLE 3.** Comparison of unit-cell parameters for different "topaz-OH" samples

| Sample* | a (Å) | b (Å) | c (Å) |
|---|---|---|---|
| UHP 270 | 4.7281(1) | 8.9326(2) | 8.4277(1) |
| UHP 479 | 4.7247(2) | 8.9258(2) | 8.4255(2) |
| UHP 270** | 4.7281(1) | 8.9318(3) | 8.4280(3) |
| Single crystal | 4.7238(30) | 8.9473(69) | 8.3900(77) |

* Cf. footnotes to Table 1.
** From Rietveld refinement. ESD factor applied (cf. Bérar and Lelann, 1991).

h (Table 1) have single crystals of "topaz-OH" large enough for single-crystal studies (200 $\mu$m) been obtained. Chemical analysis by microprobe (at Bochum) of these crystals yielded a structural formula (on the basis of six O atoms, and assuming two OH pfu) $Al_{2.07(3)}Si_{0.94(3)}O_4(OH)_2$ i.e., a deficit in Si and excess in Al. Although this topaz coexists with Mg-rich phases, and small Mg contents have been reported from natural topaz (Gübelin et al., 1986), the Mg content of the synthetic crystals amounts to less than 0.01 Mg pfu. As pointed out above, the largest uncertainty in the above formula is in the actual OH content of these crystals. However, it will be discussed below that the single-crystal structure analysis did not yield evidence for significant amounts of excess OH.

The question of space group is critical for the characterization of "topaz-OH," since a reduction in symmetry (from *Pbnm* to *P*1, ascribed to ordering of OH) has been observed in OH-rich natural topaz (e.g., Akizuki et al., 1979; Parise et al., 1980). Therefore, the single crystals have been investigated in detail by Weissenberg and precession techniques, using long exposures. Photographs of the $a^*b^*$ layer and the $h01$, $0k1$ layers by the Weissenberg technique for one crystal and the $a^*b^*$ layer and the $c^*[hh0]^*$ layer by the precession technique for a second crystal did not show any reflections that would violate the space group *Pbnm*.

**TABLE 4.** Results of single-crystal X-ray diffraction: refined unit-cell parameters, atomic positions, and thermal parameters for synthetic "topaz-OH"

Space group *Pbnm*
Unit-cell parameters: $a$ = 4.7238(30) Å; $b$ = 8.9473(69) Å; $c$ = 8.3900(77) Å
$R$ = 0.046; $R_w$ = 0.045; $N$ = 865 observations
Statistical $1/\sigma_F^2$ weighting

**Atomic positions**

| Atom | site | sym. | x/a | y/b | z/c | $U_{eq}$ (×10⁴) |
|---|---|---|---|---|---|---|
| Al | 8d | 1 | −0.0948(2) | 0.1322(1) | 0.0798(1) | 108(2) |
| Si | 4c | ..*m* | 0.4019(2) | −0.0595(1) | ¼ | 108(2) |
| O1 | 4c | ..*m* | −0.2897(5) | 0.0261(2) | ¼ | 111(5) |
| O2 | 4c | ..*m* | 0.0554(5) | 0.2558(2) | ¼ | 120(5) |
| O3 | 8d | 1 | 0.2142(3) | −0.0069(2) | 0.0940(2) | 113(4) |
| OH | 8d | 1 | −0.4103(4) | 0.2508 | 0.0665(2) | 132(4) |

**Anisotropic thermal parameters (all values × 10⁴)**

| Atom | $U_{11}$ | $U_{22}$ | $U_{33}$ | $U_{23}$ | $U_{13}$ | $U_{12}$ |
|---|---|---|---|---|---|---|
| Al | 98(3) | 89(3) | 137(3) | 0(2) | 2(2) | 2(2) |
| Si | 90(3) | 88(4) | 145(4) | — | — | 0(3) |
| O1 | 88(8) | 95(9) | 150(9) | — | — | −6(8) |
| O2 | 108(10) | 102(9) | 150(9) | — | — | −3(7) |
| O3 | 101(6) | 100(6) | 136(6) | 0(5) | 6(5) | 10(5) |
| OH | 106(6) | 122(7) | 167(6) | 16(5) | 1(6) | 21(6) |

**TABLE 5.** Bond lengths, bond angles, and polyhedral distortion parameters in the crystal structure of topaz

| | $X_{OH}$ = 1.0 | $X_{OH}$ = 0.28 |
|---|---|---|
| [4]Si-O1 | 1.646(3) Å | 1.637(1) Å |
| O2 | 1.665(2) Å | 1.651(1) Å |
| O3 (×2) | 1.649(2) Å | 1.643(1) Å |
| Average value | 1.652 | 1.644 |
| O1-Si-O2 | 110.8(1)° | 110.6(1)° |
| O1-Si-O3 (×2) | 110.1(1)° | 109.8(<1)° |
| O2-Si-O3 (×2) | 110.4(1)° | 109.8(<1)° |
| O3-Si-O3′ | 105.0(1)° | 107.0(1)° |
| p.v. | 2.311(5) Å³ | 2.277(3) Å³ |
| q.e. | 1.001(2) | 1.000(1) |
| a.v. | 4.961 | 1.747 |
| [6]Al-O1 | 1.946(2) Å | 1.908(1) Å |
| O2 | 1.940(2) Å | 1.911(1) Å |
| O3 | 1.922(2) Å | 1.902(1) Å |
| O3′ | 1.924(2) Å | 1.894(1) Å |
| OH/F | 1.833(2) Å | 1.802(1) Å |
| OH/F′ | 1.834(2) Å | 1.808(1) Å |
| Average value Al-O | 1.933 | 1.904 |
| Average value Al-OH/F | 1.834 | 1.805 |
| O1-Al-O2 | 84.9(1)° | 83.7(1)° |
| O1-Al-O3 | 89.9(1)° | 91.4(<1)° |
| O1-Al-O3′ | 97.7(1)° | 99.9(<1)° |
| O1-Al-OH/F | 86.7(1)° | 88.0(<1)° |
| O2-Al-O3 | 92.6(1)° | 94.8(<1)° |
| O2-Al-OH/F | 90.7(1)° | 90.5(<1)° |
| O2-Al-OH/F′ | 89.6(1)° | 89.2(1)° |
| O3-Al-O3′ | 83.8(1)° | 83.2(<1)° |
| O3-Al-OH/F′ | 92.9(1)° | 91.8(<1)° |
| O3′-Al-OH/F | 93.0(1)° | 91.6(<1)° |
| O3′-Al-OH/F′ | 88.0(1)° | 87.3(1)° |
| OH/F-Al-OH/F′ | 90.0(1)° | 89.4(<1)° |
| p.v. | 9.083(15) Å³ | 8.654(9) Å³ |
| q.e. | 1.005(1) | 1.007(1) |
| a.v. | 14.872 | 20.611 |

*Note:* Data for "topaz-OH" ($X_{OH}$ = 1.0, see Table 4) are compared with parameters in F-rich topaz [OH/(F + OH) = 0.28] (Zemann et al. 1979); p.v. = polyhedral volume, q.e. = quadratic elongation, a.v. = angle variance (Hazen and Finger, 1982).

The final refined atomic positions, along with the refinement indices and the refined anisotropic thermal factors are listed in Table 4, and derived bond lengths and angles are given in Table 5. Table 5 also contains the corresponding values from the neutron diffraction refinement by Zemann et al. (1979) of OH-rich [OH/(OH + F) = 0.28] topaz. Observed and final calculated structure factors are found in Table 6.[1] The X-ray powder Rietveld refinement of sample UHP270 (cf. Table 1) yielded, within the precision of the measurements, identical results for atomic positions, but different lattice constants (Table 3). The implications of the crystal structure determination will be discussed below.

## Morphology and twinning

The synthetic products consist of well-developed idiomorphic single crystals and twin aggregates up to 200 $\mu$m

[1] A copy of Table 6 may be ordered as Document AM-93-520 from the Business Office, Mineralogical Society of America, 1130 Seventeenth Street NW, Suite 330, Washington, DC 20036, U.S.A. Please remit $5.00 in advance for the microfiche.

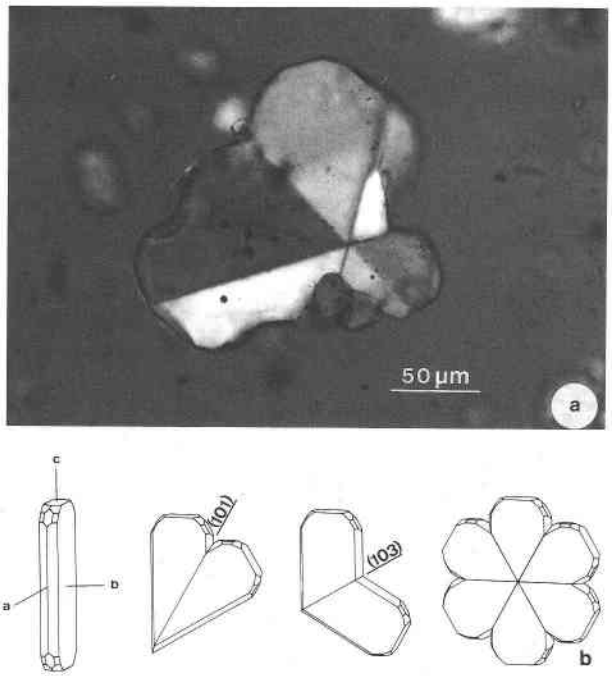


Fig. 4. Morphology of synthetic "topaz-OH." (**a**) Photomicrograph of a cyclic twin. (**b**) Idealized drawing of a single crystal and different types of twins (single crystal in normal orientation, twins are seen in a direction nearly parallel to the **b** axis).

in diameter (Fig. 4). In contrast to the habit of natural crystals (see below), they are platy with dominant {010} faces. The twins resemble very much the well-known elbowlike contact twins or cyclic twins of chrysoberyl. Twin planes (101) and (103) were confirmed by combined optical and X-ray single-crystal studies.

### Optical properties

The measured optical data of "topaz-OH" are as follows: $n_x \parallel a = 1.700(1)$, $n_y \parallel b = 1.701(1)$, $n_z \parallel c = 1.703(1)$, $\Delta n = 0.0040(5)$, and $2V_\gamma = 28(2)°$.

The Gladstone-Dale relationship can be used to assess the consistency of the refractive index, the chemical formula, and the density (Mandarino, 1976; Eggleton, 1991). Based on the cell dimensions reported above and the structural formula $Al_{1.99}Si_{0.99}O_{3.93}(OH)_{2.07}$ (6O) derived for the material synthesized in the $Al_2O_3$-$SiO_2$-$H_2O$ system, the calculated density of "topaz-OH" is $D = 3.350$ g/cm³, whereas for the ideal formula $Al_2SiO_4(OH)_2$ the density would be 3.359 g/cm³. With the new Gladstone-Dale constant for $^{[6]}Al_2O_3$ (Eggleton, 1991), both density values lead to a $K_p/K_c - 1$ parameter (Mandarino, 1979) of 0.006, which indicates good consistency among structural formula, density, and mean refractive index (category "superior" according to Mandarino, 1979).

### Infrared absorption

The infrared spectra of two different synthetic "topaz-OH" samples (synthesized at 1000 °C, 90 kbar, from the $Al_2SiO_5$ gel and at 900 °C, 100 kbar, from the $Al_2SiO_5$ + excess $SiO_2$ composition, respectively) in the region of $H_2O$ stretching vibrations are compared with that of an OH-bearing but F-rich natural topaz in Figure 5. These differ essentially with respect to two features: whereas the natural F-rich topaz shows one sharp OH vibration at 3640 cm⁻¹, two bands appear in the spectrum of "topaz-OH," a rather sharp one at 3600 cm⁻¹ and a much broader one, with a pronounced tail toward lower wavenumbers, having a maximum absorption near 3520 cm⁻¹. The two spectra of "topaz-OH," on the other hand, are very similar, as they only differ with respect to the relative intensities of the two bands.

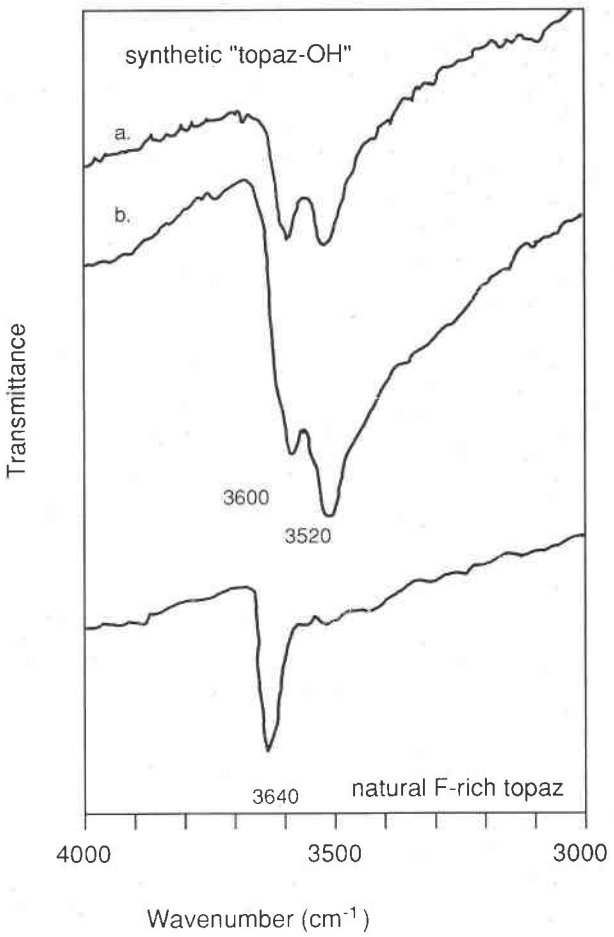


Fig. 5. Infrared absorption spectra of a natural F-rich topaz (bottom) compared with those of synthetic "topaz-OH" (top, a: synthesized from excess $SiO_2$ composition, fourth experiment in Table 1; b: synthesized from $Al_2SiO_5$-gel, sixth experiment in Table 1) in the region of OH stretching frequencies. Note the presence of at least two bands in the spectra of "topaz-OH" and the pronounced shoulders toward lower wavenumbers.

## Discussion

### Crystal structure

The synthesis of end-member "topaz-OH" has been surprising, because several authors (Parise et al., 1980;

Barton, 1982) had suggested that the topaz structure should be destabilized by OH/(OH + F) > 0.5, this destabilization being caused by mutual repulsion of H atoms forced to be in proximity (~1.5 Å) to each other. Energy calculations by Abbott (1990) suggest that this destabilization can be avoided if the H atoms are allowed to move off the positions found by Zemann et al. (1979) for OH-rich topaz [OH/(OH + F) = 0.28] and form H bonds bridging the OH-OH edge of the $AlO_4(OH)_2$ octahedron, even though this would result in short Al-H distances.

As evident from the bond-length, bond-angle, and site-distortion parameters listed in Table 5, the structure of pure "topaz-OH" is similar to the predominantly F-bearing structure reported by Zemann et al. (1979). However, both the Al and Si sites are larger in "topaz-OH" than those found in fluorine topaz, amounting to a volume expansion of 5% for the Al site and of 1.5% for the Si site. The distortion measures of the sites (quadratic elongation and angle variance) show that although the differences between the two structures are significant, they are not as large as might be expected, given the difference in chemistry. In detail, the Si site of "topaz-OH" is slightly more distorted than that of F-rich topaz, and the Al site of "topaz-OH" is slightly less distorted than that of F-rich topaz, based on the measure of angle variance. Individual bond lengths show the same results. Not surprisingly, the strong Si-O bonds are changed less than 1% by the OH-F interchange; note that this expansion is discordant with the observation of Ohashi (1982) that Si-O distances in topaz tend to increase with F content. The bond lengths around Al also show significant (~0.03 Å) changes; however the volume expansion by the substitution of OH for F seems to be primarily one of dilatation, i.e., the Al-OH bonds (in normal topaz, primarily Al-F) are no more affected than the remaining four bonds.

H can be very difficult to locate in any X-ray crystal structure refinement, and, in fact, no evidence for H was found in the Fourier difference maps determined by the final refined parameters. An attempt to predict the location of H on the basis of stereochemical considerations failed as well. Using the bond-length–bond-strength data of Brown and Altermatt (1985) on bond length and bond strength, we find that the valence sums to O are 1.84 vu to O1, 1.81 vu to O2, 1.89 vu to O3, and 1.22 vu to the O in the OH site (exclusive of bonds to H). The 0.78 vu underbonding of that O must reflect the H forming a strong O-H bond. This also leaves the possibility of forming a moderately strong (0.22 vu) H···O H bond with another O, which however could not be identified.

In summary, the distribution of H in the unit cell is not revealed by the structural refinement, and no straightforward solution is offered by stereochemical considerations. The lack of an obvious H-bond acceptor O is consistent with the previously noted lack of marked structural change relative to fluorine topaz, in which, of course, there are no H bonds. The two primary questions remaining in regard to the crystal structure of "topaz-OH" are (1) what is the H bonding scheme, and (2) why is the distortion of the $AlO_4(OH,F)_2$ polyhedron so little affected by the substitution?

### Unit-cell parameters

Figure 6 is a plot of the unit-cell parameters and unit-cell volume of natural topaz as a function of OH content and compares them with the data of the synthetic OH end-member described here. The lines are fits to the F-bearing samples only. For the *a* and *b* unit-cell parameters and the unit-cell volume, there appears to be a fairly linear trend of parameter vs. OH content for OH/(OH + F) < 0.3 (cf. Ribbe and Rosenberg, 1971), and these seem to continue toward the OH end-member, but the relationship cannot be linear over the entire compositional range. On the other hand, there is no clear trend discernible for the *c* parameter in the high-F natural samples, and there are large differences in *c* between the "topaz-OH" sample used for single-crystal structure analysis and the other samples. These latter differences with respect to the *c* parameter are particularly intriguing, as there is no evidence for other structural differences. The major distinction between these two samples is that the single crystal was grown under silica-undersaturated conditions, whereas the powder samples were synthesized on "topaz-OH" composition, or under silica-saturated conditions. Such chemical differences are also evident from the analyzed Al:Si ratios reported above.

### Infrared data

Although topaz containing OH and F of orthorhombic symmetry should only exhibit one OH species and one IR stretching mode, it is well known from studies of natural topaz that, in addition to the 3650-$cm^{-1}$ band ascribed to normal structural OH, anomalous peaks may appear in the region 3460–3400 $cm^{-1}$ (Aines and Rossmann, 1985, 1986). These bands, which are invariably much weaker than the main OH band, seem to be associated with structural defects, as the OH causing the anomalous peaks converts to normal OH at elevated temperatures, but the nature of the defects is not clear at the moment. It should also be pointed out that topaz containing OH and F synthesized by Rosenberg (1972) shows, in the infrared spectra, extended tails toward lower frequencies.

Our observation of two IR bands, both ascribed to stoichiometric OH and with similar intensities (at 3600 and 3520 $cm^{-1}$, i.e., outside the range of defect bands mentioned above) can be rationalized as either a lowering of overall symmetry or a splitting of nondegenerate vibrations. Lowering of symmetry to any of the translation-equivalent subgroups of *Pbnm* listed in International Tables vol. A (1983) would split the single OH site (site symmetry 1) into two sites with distinct symmetry, with, therefore, potentially different O-H vibrational frequencies. There is no X-ray crystallographic evidence and no particular crystal-chemical necessity for lower symmetry; however, the acentric space group $Pbn2_1$ has the same

systematic extinctions as *Pbnm* and could only be detected conclusively by a center-of-symmetry test, e.g., second-harmonic generation or optical activity.

The second possible explanation for doubling of the OH band (dynamic change in symmetry) is splitting of the nondegenerate OH vibrations, i.e., Davydov splitting (Lazarev, 1974). In the topaz unit cell, all eight OH groups are translationally inequivalent; however, they may (from the orientation of the O-H vector) be roughly divided into two classes of four OH groups each. Interactions among OH groups in these classes (essentially between OH groups related by the ($x$, $y$, 0.25) or ($x$, $y$, 0.75) mirror planes, which have H-H distances of only 1.48 Å) are likely to be strong and may be sufficient to cause splitting of the OH vibrational line. This splitting is caused by coupling between the vibrations of the two OH groups, which yields, instead of a single frequency, two vibrational frequencies corresponding to the vector sum and difference of the transient intermolecular dipoles. Further splitting caused by the nonequivalence of the four OH groups in each class is probably too minor to be observed, in part because interactions among these OH groups are likely to be weak because of the large interatomic distances involved.

Despite these uncertainties in the origin of the two IR bands, it is clear that the frequency of the O-H stretching mode of the OH site decreases from OH-poor to OH-rich topaz and that, therefore, the O-H$\cdots$O distance should decrease as well (Nakamoto et al., 1955).

### Variation of optical properties with composition

As known from the work of Ribbe and Rosenberg (1971), the optical constants of natural topaz crystals represent a very useful tool for the quick and precise determination of F content. In particular, the $2V$ values can easily be derived from the perfectly centered axial figures of cleavage flakes (001). Comparing the optical axial angle data for F-rich topaz to the value for "topaz-OH" (Fig. 7) reveals that the latter clearly falls off the linear trend observed in F-rich topaz. Thus, the Ribbe and Rosenberg equations only hold for F-dominant topaz and cannot be extrapolated toward the OH end-member.

### General discussion of the "topaz-OH" structure

The structural data discussed above demonstrate that the material synthesized corresponds to the OH end-member of the solid solution of fluorine and hydroxyl topaz. Certain aspects of the crystal chemistry and properties (e.g., nonstoichiometry and its influence on lattice constants) require further investigation. However, some of the results (such as the almost purely dilatational expansion of the structure by the OH for F substitution, lack of evidence for the position of H, split OH-bands in the infrared spectrum, anomalous optical properties) suggest that our fundamental view of the structure (as determined at room temperature and 1 bar) is inadequate or at least incomplete. In view of the fact that "topaz-OH" is metastable under these conditions and that many very high-pressure silicate phases cannot be quenched to 1 bar (some even transforming to glassy states), it seems possible that "topaz-OH" has also undergone minor structural changes during decompression. In that case the

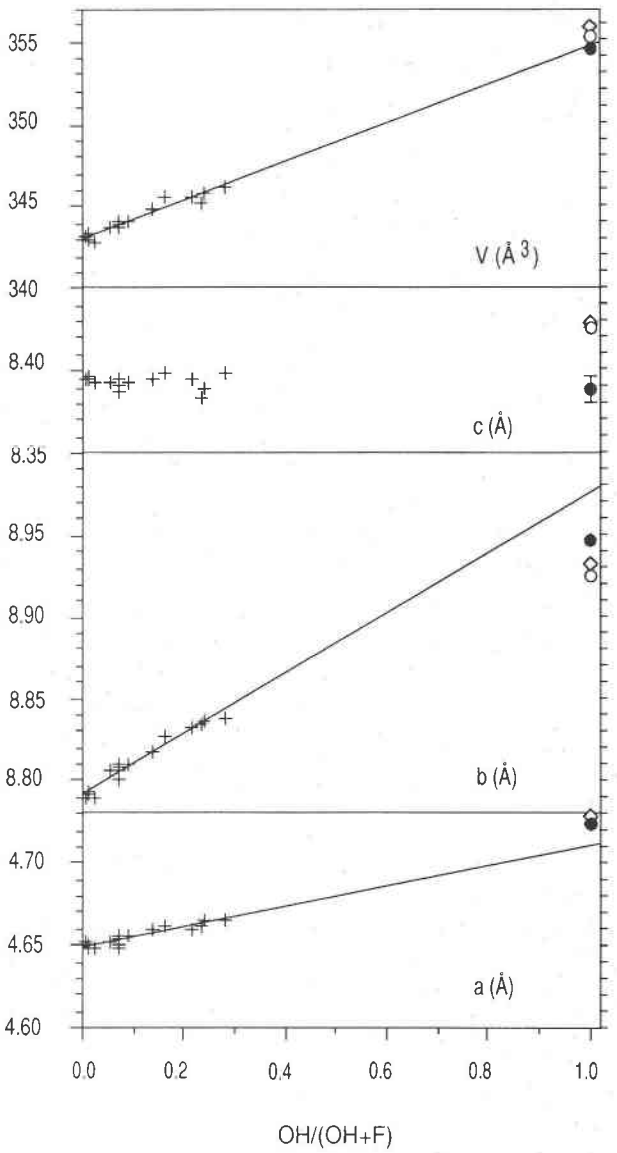


Fig. 6. Correlation between $X_{OH}$ and lattice constants in natural topaz and synthetic "topaz-OH." Data taken from Rosenberg (1967) and Ribbe and Rosenberg (1971), supplemented by data from Barton et al. (1982), Gübelin et al. (1986), and Zemann et al. (1979). For internal consistency, all analyses have been recalculated on the basis of the analyzed F content only, assuming (OH + F) = 2 pfu. Results of this study at OH/(F + OH) = 1.0 are given by the diamonds (sample UHP 270), open circles (sample UHP 479), and solid circles (single crystal, cf. Table 4). The diamonds and circles are larger than their respective ($\pm 1\sigma$) error bars. Only the error bar for the $c$ parameter of the single-crystal data is indicated. Regression lines are based on the data for natural topaz only, and they indicate nonlinearities in the variation of lattice parameters $a$ and $b$ across the binary join.

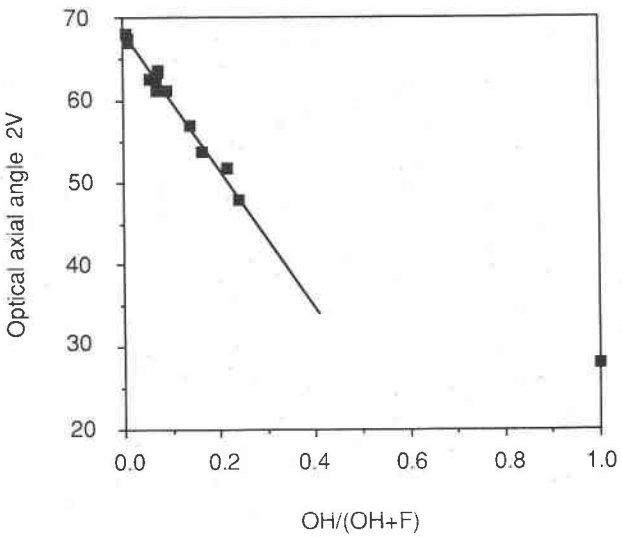


Fig. 7. Relationship between OH/(OH + F) ratio and optical axial angle $2V$ in topaz. Data for F-rich natural topaz taken from Rosenberg (1967) and Ribbe and Rosenberg (1971); those for "topaz-OH" are from this study. Note that the regression line to the F-rich data does not pass through the OH/(OH + F) = 1.0 point.

structural properties measured at room temperature and 1 bar may not correspond closely to those that obtain at the conditions of synthesis; furthermore, the observations might be found to be somewhat at variance with notions of proper crystal chemistry, which is based (in large part) on observations of materials in a more nearly stable state. As a specific instance of this problem, Hartree-Fock band structure calculations by Sherman (1991) on structures in the $Al_2O_3$-$SiO_2$-$H_2O$ system indicate that H bonding might be strengthened at high pressures. If this observation holds for "topaz-OH," then the impossibility of locating the protons in the (1-bar) crystal structure may be the result of a change in the bonding environment with change in pressure and not due to any inherent disorder of protons in the structure under conditions of synthesis.

## Twinning

Reports of twinning in natural topaz crystals are rare. The only published report of contact twins with a twin plane (101), as observed in the synthetic "topaz-OH," has been that of Goldschmidt (1910) on topaz of unknown composition from an unknown locality in Brazil. However, twinned topaz crystals from natural occurrences have been found contemporaneously with the present investigation of the synthetic OH end-member. They are rock-forming minerals in two occurrences of high-pressure, low-temperature metamorphic rocks from Crete (Fig. 8). The metamorphic conditions of these rocks were 300–350 °C at 9–10 kbar, and the topaz crystals are among the most OH-rich topaz (OH/[OH + F] = 0.33, Theye, 1990 personal communication) known so far from natural rocks.

Von Gliszcynski (1949) discussed the topaz structure in detail with respect to possible twinning and concluded

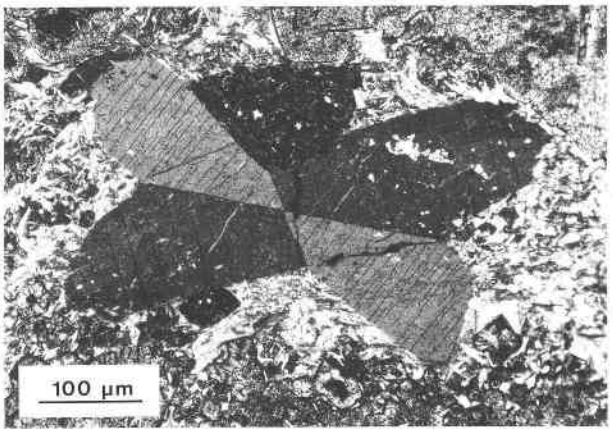


Fig. 8. Photomicrograph of a twinned topaz crystal in thin section of a metabauxite sample from Sisses, Crete. Sample courtesy of T. Theye, Bochum.

that the difference between the 57°58′ angle of the $c$ axes of two individuals twinned after (101) and the pseudo-hexagonal angle of 60° is too large to allow the formation of penetration twins, and, at best, contact twins as described by Goldschmidt (1910) are possible. Following this argument, the preferential twinning in "topaz-OH" can easily be explained: the lattice constants $a$ and $c$ of "topaz-OH" lead to a twin angle of 58°36′, which is a closer approach to the theoretically required 60° than for F-rich topaz. Most probably, twinning will become a diagnostic feature for OH-rich topaz that is especially likely to occur in high-pressure metamorphic rocks.

## Implications for the thermodynamic model of the OH-F topaz solid-solution series

The implications of the single-crystal structure analysis and of the variation of the lattice constants for solid solution between topaz and "topaz-OH" seem clear, at least in part. A wide range of solid solution between the two end-members may well be possible. Although the variation of the $c$ cell parameter with OH content remains ambiguous, the $a$ and $b$ parameters are at least principally concordant with trends seen for F-rich topaz. It is, of course, entirely possible that some aspects of the thermodynamics of mixing of the two end-members could result in a miscibility gap in the phase diagram, but some substitution of F into "topaz-OH" should be possible at elevated pressure. On the other hand, the differences in unit cell between topaz samples synthesized under differing conditions of silica saturation are significant and suggest that some important details of the thermodynamic behavior of this phase are not yet completely understood.

In his careful study of OH-F exchange of topaz in equilibrium with andalusite and vapor, Barton (1982) demonstrated that $X_{OH}$ increases with decreasing temperatures and increasing $H_2O$ pressures and that the experimental data could be fitted within the uncertainties by both an ideal mixing model and a proton-avoidance model. He chose the proton-avoidance model, which im-

plies that $X_{OH}$ can never exceed 0.5, mostly because the ideal model would predict the formation of the pure "topaz-OH" end-member at the expense of andalusite and $H_2O$ vapor, in contradiction to natural assemblages.

The synthesis of the pure OH end-member clearly indicates that the proton-avoidance model for the activity-composition relationships in the topaz solid solution cannot be correct. On the other hand, an improved model can only be established after the role of OH in the crystal structure and its order-disorder relationship with F are better constrained.

With respect to the pressure dependence of the solid solubility between the F and OH end-members, striking similarities exist between topaz and the humite group of minerals in the system $Mg(OH)_2$-$MgF_2$-$SiO_2$ (cf. review by Ribbe, 1982b). In both cases, the F end-members are stable at 1 bar pressure, and under conditions of the Earth's crust the substitution of OH for F is limited (Duffy and Greenwood, 1979). Proton-proton repulsion has been made responsible for this pressure-dependence in the humite group (Van Valkenburg, 1961; Ribbe, 1982b), as for topaz (see above). High pressures are obviously necessary to overcome this proton-proton repulsion, since both OH end-member humite group minerals (Yamamoto and Akimoto, 1977) and "topaz-OH" become stable phases only at pressures corresponding to mantle depths. However, unlike topaz, in which the cationic substitutions are limited, the OH end-members of the humite group minerals may also be stabilized at lower pressures by substitutions in cationic sites (e.g., Mn, Cd, Ge; see Ribbe, 1982b).

## Petrological application

In Figure 9 the dehydration curve "topaz-OH" = kyanite + $H_2O$ is compared with hypothetical linear geotherms calculated using a mean density of 3.3 g/cm$^3$, with the continental geotherm caused by a heat flow of 40 mW/m$^2$, as well as with the relevant polymorphic transitions of $SiO_2$ and C. It is clear that there is no overlap of "topaz-OH" stability with $P$-$T$ conditions prevailing in the subcontinental lithosphere, from which xenoliths of mantle peridotites and eclogites are believed to have been derived (Dawson and Carswell, 1990). This is in agreement with the consistent occurrence of kyanite as the only aluminum silicate in these xenoliths. Topaz was once reported as an inclusion in diamond by Dumas (1840), but Meyer (1987) considered that to be a misidentification.

On the other hand, "topaz-OH" might be an important mineral in deeply subducted Al-rich pelitic sediments. According to Peacock (1990a), the $P$-$T$-$t$ paths of subducting slabs show curvatures during subduction toward progressively colder geotherms. Thus, for long-lasting subduction, the top of a slab carried down into an old subduction zone may only reach temperatures of about 600 °C at pressures of 50 kbar (Peacock, 1990a, his Fig. 5). $P$-$T$ combinations of this type follow approximately the linear geotherm of 4 °C/km shown in Figure 9. This

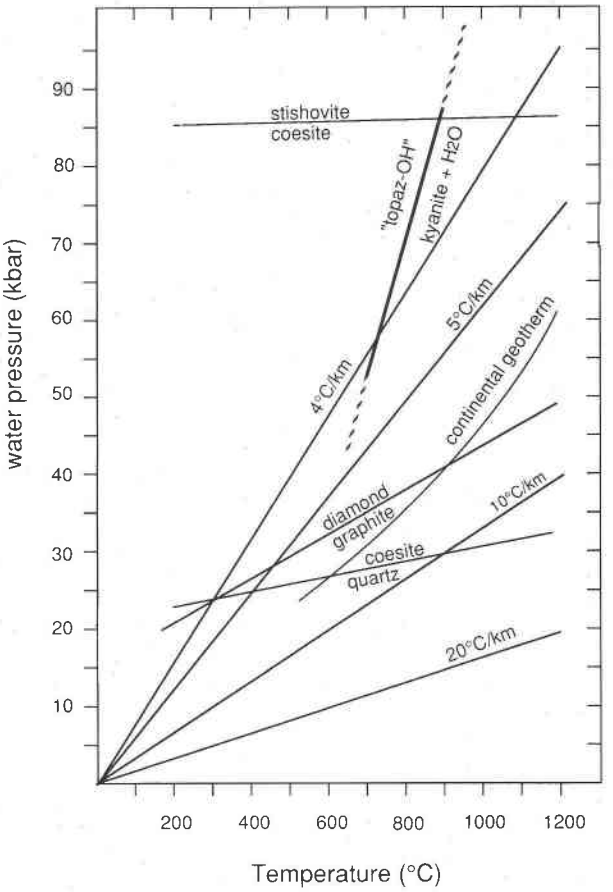


Fig. 9. Comparison of the high-temperature stability limit of "topaz-OH" (heavy line) with stability limits in the $SiO_2$ and C systems and geothermal gradients. Note that the linear geotherm at 4 °C/km intersects the topaz = kyanite + vapor reaction curve. For further discussion see text.

means that sediments still present at the top of the subducting slab would pass the stability field of "topaz-OH" near 50–60 kbar and 600–750 °C (Fig. 9), which translates into depths of about 175 km. In this case, "topaz-OH" may appear at least as a transient phase, before still deeper subduction, or a temperature increase at the end of subduction, takes place and leads to its dehydration and the formation of kyanite. Obviously, this model would apply also to aluminous, possibly diamondiferous eclogites in these cold subduction zones, so that the kyanite found in many of these ultra-high-pressure eclogite xenoliths (Dawson and Carswell, 1990) might in fact have formed from preexisting "topaz-OH."

In their thermodynamic analysis of phase relations in the $Al_2O_3$-$SiO_2$-$H_2O$ system at high pressures and low temperatures, Delany and Helgeson (1978) show that the hydrous assemblage diaspore + $SiO_2$ (quartz or coesite) persists up to at least 50 kbar, 500 °C. Peacock (1990b), using the more recent data set of Berman (1988), calculated breakdown of this pair to form kyanite + $H_2O$ for the 50–60 kbar at about 430–450 °C, which would mean

complete dehydration for all compositions of the $Al_2O_3$-$SiO_2$-$H_2O$ system between kyanite and $SiO_2$.

With the finding of the new high-pressure phase "topaz-OH" reported here, as well as with the approximate knowledge of the stability of phase Pi (Coes, 1962; Wunder and Schreyer, 1991), it is clear that the assumed complete dehydration of $SiO_2$-rich compositions in the $Al_2O_3$-$SiO_2$-$H_2O$ system does not occur at the low temperatures indicated. Rather, diaspore + $SiO_2$, which was actually found in natural metamorphic rocks (De Roever, 1947; Theye and Ockenga, 1988, and personal communication), will react without participation of $H_2O$ to form phase Pi, which in turn will subsequently form "topaz-OH" through reaction with diaspore, again conserving the $H_2O$ content of the system (see Fig. 1). It is thus clear that, with the new experimental results, the capacity of aluminous rocks to retain $H_2O$ within their crystalline phases is extended to much higher temperatures. Compared with the deductions by Peacock (1990b), the temperature increase necessary for dehydration at 60 kbar amounts to some 300 °C.

## Acknowledgments

We thank Peter Daniels, Bochum, for performing the single-crystal X-ray data collection, George Rossman, Pasadena, and Josef Zemann, Vienna, for helpful discussions, and H. Küfner, Bayreuth, for technical assistance. This work has been supported by grants from Deutsche Forschungsgemeinschaft, Bonn, and Fonds der Chemischen Industrie, Frankfurt, to F.S., and it is part of the research conducted at Bochum under the auspices of the DFG-Forschergruppe Hochdruck-Metamorphose in Natur und Experiment. The constructive help of J.A. Mandarino in the nomenclature discussion is much appreciated.

## References cited

Abbott, R.N., Jr. (1990) Topaz: Energy calculations bearing on the location of hydrogen. Canadian Mineralogist, 28, 827–834.

Aines, R.D., and Rossman, G.R. (1985) The high temperature behavior of trace hydrous components in silicate minerals. American Mineralogist, 70, 1169–1179.

——— (1986) Relationships between radiation damage and trace water in zircon, quartz, and topaz. American Mineralogist, 71, 1186–1193.

Akizuki, M., Hampar, M.S., and Zussman, J. (1979) An explanation of anomalous optical properties of topaz. Mineralogical Magazine, 43, 237–241.

Barton, M.D. (1982) The thermodynamic properties of topaz solid solutions and some petrologic applications. American Mineralogist, 67, 956–974.

Barton, M.D., Haselton, H.T., Jr., Hemingway, B.S., Kleppa, O.J., and Robie, R.A. (1982) The thermodynamic properties of fluor-topaz. American Mineralogist, 67, 350–355.

Bérar, J.F., and Lelann, P. (1991) E.S.D.'s and estimated probable error obtained in Rietveld refinements with local correlations. Journal of Applied Crystallography, 24, 1–5.

Berman, R.G. (1988) Internally-consistent thermodynamic data for minerals in the system $Na_2O$-$K_2O$-CaO-MgO-FeO-$Fe_2O_3$-$Al_2O_3$-$SiO_2$-$TiO_2$-$H_2O$-$CO_2$. Journal of Petrology, 29, 445–522.

Boyd, F.R., and England, J.L. (1960) Apparatus for phase-equilibrium measurements at pressure up to 50 kilobars and temperatures up to 1750 °C. Journal of Geophysical Research, 65, 741–748.

Brown, I.D., and Altermatt, D. (1985) Bond-valence parameters obtained from a systematic analysis of the inorganic crystal structure database. Acta Crystallographica, 41B, 244–247.

Canil, D. (1991) Experimental evidence for the exsolution of cratonic lherzolite from high temperature harzburgite. Earth and Planetary Science Letters, 106, 64–72.

Coes, L., Jr. (1962) Synthesis of minerals at high pressures. In R. Wentorf, Ed., Modern very high pressure techniques, p. 137–150. Butterworths, London.

Dawson, J.B., and Carswell, D.A. (1990) High temperature and ultrahigh-pressure eclogites. In D.A. Carswell, Ed., Eclogite facies rocks, p. 315–349. Blackie, London.

Day, H.W. (1972) Geometrical analysis of phase equilibria in ternary systems of six phases. American Journal of Science, 272, 711–734.

Delany, J.M., and Helgeson, H.C. (1978) Calculation of thermodynamic consequences of dehydration in subducting oceanic crust to 100 KB and >800 °C. American Journal of Science, 278, 638–686.

De Roever, W.P. (1947) Igneous metamorphic rocks in eastern central Celebes. In H.A. Brouwer, Ed., Geological explorations in the island of Celebes, p. 65–173. North Holland, Amsterdam.

Duffy, C.J., and Greenwood, H.J. (1979) Phase equilibria in the system MgO-$MgF_2$-$SiO_2$-$H_2O$. American Mineralogist, 64, 1156–1174.

Dumas, A. (1840) Recherches sur la véritable poids atomique du carbonne. Comptes Rendues Academie des Sciences, 11, 991.

Eggleton, R.A. (1991) Gladstone-Dale constants for the major elements in silicates: Coordination number, polarizability, and Lorentz-Lorentz relation. Canadian Mineralogist, 29, 525–532.

Eggleton, R.A., Boland, J.N., and Ringwood, A.E. (1978) High pressure synthesis of a new aluminium silicate: $Al_5Si_5O_{17}(OH)$. Geochemical Journal, 12, 191–194.

Gebert, W., and Zemann, J. (1965) Messung des Ultrarot-Pleochroismus von Mineralen. III. Der Pleochroismus der OH-Streckfrequenz in Topas. Neues Jahrbuch für Mineralogie Monatshefte, 380–384.

Goldschmidt, V. (1910) Topaszwillinge aus Brasilien. Zeitschrift für Kristallographie, 47, 639–644.

Gübelin, E., Graziani, G., and Kazmi, A.H. (1986) Pink topaz from Pakistan. Gems and Gemology, 22, 140–151.

Hamilton, D.L., and Henderson, C.M.B. (1968) The preparation of silicate compositions by a gelling method. Mineralogical Magazine, 36, 832–838.

Hazen, R.M., and Finger, L.W. (1982) Comparative crystal chemistry, 231 p. Wiley, New York.

International Tables for Crystallography, Volume A (1983), Reidel, Dordrecht, The Netherlands.

Ito, E., Takahashi, E., and Matsui, Y. (1984) The mineralogy and chemistry of the lower mantle: An implication of the ultra-high pressure phase relations in the system MgO-FeO-$SiO_2$. Earth and Planetary Science Letters, 67, 238–248.

Kanzaki, M. (1987) Physical properties of silicate melts at high pressures. Ph.D. thesis, Geophysical Institute, University of Tokyo.

Lazarev, A.N. (1974) The dynamics of crystal lattices. In V.C. Farmer, Ed., The infrared spectra of minerals, p. 69–85. Mineralogical Society, London.

Mandarino, J.A. (1976) The Gladstone-Dale relationship. I. Derivation of new constants. Canadian Mineralogist, 14, 498–502.

——— (1979) The Gladstone-Dale relationship. III. Some general applications. Canadian Mineralogist, 17, 71–76.

Massonne, H.J., and Schreyer, W. (1986) High-pressure synthesis and x-ray properties of white micas in the system $K_2O$-MgO-$Al_2O_3$-$SiO_2$-$H_2O$. Neues Jahrbuch für Mineralogie Abhandlungen, 153, 177–215.

Medenbach, O. (1985) A new microrefractometer spindle-stage and its application. Fortschritte der Mineralogie, 63, 111–133.

Medenbach, O., Schreyer, W., Wunder, B., Ross, C., Rubie, D.C., and Seifert, F. (1990) OH-topaz, a new high-pressure phase in the system $Al_2O_3$-$SiO_2$-$H_2O$ (abs.). Eos, 71, 1707–1708.

Meyer, H.O.A. (1987) Inclusions in diamonds. In P.H. Nixon, Ed., Mantle xenoliths, p. 501–522. Wiley, New York.

Nakamoto, K., Margoshes, M., and Rundle, R.E. (1955) Stretching frequencies as a function of distances in hydrogen bonds. Journal of the American Chemical Society, 77, 6480–6486.

Ohashi, H. (1982) Si-O distances in some silicates containing fluor ions. Journal of the Japanese Association of Mineralogists, Petrologists, and Economic Geologists, 77, 33–36.

Pardee, J.T., Glass, J.J., and Stevens, R.E. (1937) Massive low fluorine topaz from Brewer mine, South Carolina. American Mineralogist, 22, 1058–1064.

Parise, J.B., Cuff, C., and Moore, F.H. (1980) A neutron diffraction study

of topaz: Evidence for lower symmetry. Mineralogical Magazine, 43, 943–944.

Peacock, S.M. (1990a) Numerical simulation of metamorphic pressure-temperature-time paths and fluid production in subducting slabs. Tectonics, 9, 1197–1211.

——— (1990b) Fluid processes in subduction zones. Science, 248, 329–337.

Pyrros, N.P., and Hubbard, C.R. (1983) Rational functions as profile models in powder diffraction. Journal of Applied Crystallography, 16, 289–294.

Ribbe, P.H. (1982a) Topaz. In Mineralogical Society of America Reviews in Mineralogy, 5, 215–230.

——— (1982b) The humite series and Mn-analogs. In Mineralogical Society of America Reviews in Mineralogy, 5, 231–274.

Ribbe, P.H., and Gibbs, G.V. (1971) The crystal structure of topaz and its relation to optical properties. American Mineralogist, 56, 24–30.

Ribbe, P.H., and Rosenberg, P.E. (1971) Optical and X-ray determinative methods for fluorine in topaz. American Mineralogist, 56, 1812–1821.

Rosenberg, P.E. (1967) Variations in the unit-cell dimensions of topaz and their significance. American Mineralogist, 52, 1890–1895.

——— (1972) Compositional variations in synthetic topaz. American Mineralogist, 57, 168–187.

Schreyer, W., Maresch, W.V., and Baller, T. (1991) A new hydrous, high-pressure phase with a pumpellyite structure in the system $MgO$-$Al_2O_3$-$SiO_2$-$H_2O$. In L.L. Perchuk, Ed., Progress in metamorphic and magmatic petrology, p. 47–64. Cambridge University Press, Cambridge, U.K.

Sheldrick, G.M. (1976) SHELX76, Program for crystal structure determination. University of Cambridge, England.

Sherman, D.M. (1991) Hartree-Fock band structure, equation of state, and pressure-induced hydrogen bonding in brucite, $Mg(OH)_2$. American Mineralogist, 76, 1769–1772.

Theye, Th., and Ockenga, A. (1988) Diaspor + Quarz in Metabauxiten von Amorgos (Kykladen, Griechenland). Fortschritte der Mineralogie, 66, 156.

Van Valkenburg, A. (1961) Synthesis of the humites $nMg_2SiO_4 \cdot Mg(F,OH)_2$. Journal of Research of the Natural Bureau of Standards, Physics and Chemistry, 65A, 415–428.

Vaughan, P.A., and Berman, R. (1963) The crystal structure of piezotite, $Al_3Si_2(OH)_3O_7$. Acta Crystallographica, 16, A13.

von Gliszcynski, S. (1949) Über gesetzmäßige Verwachsungen von Topasen. Neues Jahrbuch für Mineralogie und Geologie Monatshefte, Abteilung A, 1–23.

Wunder, B., and Schreyer, W. (1991) "Piezotit", ein stabiles wasserhaltiges Hochdruck-Al-Silikat. Berichte der Deutschen Mineralogischen Gesellschaft, Beiheft zu European Journal of Mineralogy, 3, 302.

Yamamoto, K., and Akimoto, S. (1977) The system $MgO$-$H_2O$-$SiO_2$ at high pressures and temperatures: Stability field for hydroxyl-chondrodite, hydroxyl-clinohumite and 10 Å-phase. American Journal of Science, 277, 288–312.

Zemann, J., Zobetz, E., Heger, G., and Vollenkle, H. (1979) Strukturbestimmung eines OH-reichen Topases. Österreichische Akademie der Wissenschaften, Mathematisch-Naturwissenschaftliche Klasse, 116, 145–147.

Manuscript received January 6, 1992
Manuscript accepted November 20, 1992